DALTON
FULL PAPER

Thermodynamics and kinetics of Ru^{III}(edta) as an efficient scavenger for nitric oxide in aqueous solution

Alicja Wanat,[a,b] Thorsten Schneppensieper,[a] Andrzej Karocki,[b] Grazyna Stochel *[b] and Rudi van Eldik *[a]

[a] *Institute for Inorganic Chemistry, University of Erlangen-Nürnberg, Egerlandstr. 1, 91058 Erlangen, Germany*
[b] *Department of Inorganic Chemistry, Jagiellonian University, Ingardena 3, 30-060 Krakow, Poland*

Received 11th September 2001, Accepted 17th December 2001
First published as an Advance Article on the web 22nd February 2002

The edta complex of Ru^{III} reacts very rapidly with NO in aqueous solution at pH = 5 to form a stable nitrosyl complex. The results from FT-IR (ATR) and ^{15}N-NMR studies clearly support the NO^+ character of coordinated NO, such that the nitrosyl product can be formulated as $[Ru^{II}(edta)NO]^+$. A combination of UV-Vis spectroscopy and electrochemical detection of NO was used to determine the overall equilibrium constant K_{NO} as $(9.1 \pm 1.2) \times 10^7$ M^{-1} at 25 °C and pH = 5.0. Stopped-flow kinetic studies on the reaction of acetate-buffered solutions of $[Ru^{III}(edta)H_2O]^-$ with NO gave k_{on} values two orders of magnitude lower than that reported in the literature as a result of buffer effects. The values of k_{on} determined at low and high pH, *viz.* 3.8×10^4 and 1.2×10^5 M^{-1} s^{-1}, respectively, are significantly smaller than that found at pH = 5.0, and in agreement with that observed for the substitution reactions of Ru^{III}(edta) with other entering nucleophiles. Attempts to determine k_{on} for the binding of NO to $[Ru^{III}(edta)H_2O]^-$ using laser flash photolysis failed due to the occurrence of side reactions. Under specific conditions (NO in excess and NO_2^- as impurity), the formation of the disubstituted $[Ru^{II}(edta)(NO^+)(NO_2^-)]^{2-}$ species was detected using ^{15}N-NMR spectroscopy. Laser flash photolysis of this complex leads to multiple chemical reaction steps as a result of the formation of two primary photoproducts, which decay with different rate constants to the starting complex. Possible mechanisms for these photoinduced reactions are proposed and compared to related systems reported in the literature.

Introduction

The potential application of ruthenium nitrosyl complexes as metallopharmaceuticals (*e.g.* as antitumor and antisepsis agents),[1] has generated new interest in the reactions of ruthenium(III) polyaminocarboxylate complexes with nitric oxide. Studies during the past decade have shown that the family of ruthenium(III) polyaminocarboxylate complexes satisfies most of the requirements for effective scavengers of NO in biological systems.[2–5] One of the most promising complexes appears to be $[Ru^{III}(edta)H_2O]^-$. This ethylenediaminetetraacetate ($edta^{4-}$) complex has been shown to be pentadentate in aqueous solution with the sixth coordination site being occupied by either a water molecule or a hydroxide ion.[6] In aqueous solution, the complex exists in three forms, *viz.* $[Ru^{III}(Hedta)H_2O]$, $[Ru^{III}(edta)H_2O]^-$ and $[Ru^{III}(edta)OH]^{2-}$, depending on the pH, according to eqn. 1 and 2.

$$[Ru^{III}(Hedta)H_2O] \xrightleftharpoons{K_1} [Ru^{III}(edta)H_2O]^- + H^+ \quad pK_1 = 2.4 \tag{1}$$

$$[Ru^{III}(edta)H_2O]^- \xrightleftharpoons{K_2} [Ru^{III}(edta)OH]^{2-} + H^+ \quad pK_2 = 7.6 \tag{2}$$

The pK_1 value corresponds to the deprotonation of the uncoordinated carboxylic acid group of the $Hedta^{3-}$ ligand, and the more basic pK_2 corresponds to the deprotonation of coordinated water.

Kinetic studies on the substitution behaviour of this complex revealed its extreme lability in comparison to other nonchelated complexes of Ru^{III}, with the maximum reactivity reached at $4 < pH < 6$.[6–10] This is ascribed to the participation of the very labile $[Ru^{III}(edta)H_2O]^-$ complex. Since displacement of H_2O by L (L = nucleophile) is kinetically more favourable than displacement of OH^- by L, the lower reactivity of $[Ru^{III}(edta)OH]^{2-}$ (at pH > 8) compared to $[Ru^{III}(edta)H_2O]^-$ is not surprising. However, there is no rationalisation for the low reactivity of $[Ru^{III}(Hedta)H_2O]$ compared to that of $[Ru^{III}(edta)H_2O]^-$. Matsubara and Creutz demonstrated that both a coordinated water molecule and a pendant free carboxylate arm are required for the extreme lability of $[Ru^{III}(edta)H_2O]^-$.[6] There is evidence that suggests that the maximum reactivity in this case can be ascribed to steric activation of an associative process (hydrogen bonding between coordinated water and an oxygen of the free carboxylate arm has the net effect of distorting all the metal–ligand bonds slightly, creating an accessible site for attack by the entering ligand). In order to understand this high lability, systematic kinetic studies of the substitution behaviour of this complex with a series of nucleophiles were undertaken, and the results support the operation of an associative ligand substitution mechanism.[11–13]

The thermodynamics and kinetics of the interaction of Ru^{III}(edta) with NO appears to be especially interesting from a medical, catalytic and kinetic point of view. In this respect, Davies *et al.* have studied the kinetics of NO binding to $[Ru^{III}(edta)H_2O]^-$ using stopped-flow techniques.[5] They showed that $[Ru^{III}(edta)H_2O]^-$ scavenges NO rapidly ($k = 2.6 \times 10^7$ M^{-1} s^{-1} at 7 °C) to form $[Ru^{III}(edta)NO]^-$. On the other hand, Meyer *et al.* have used $[Ru^{III}(edta)H_2O]^-$ to catalyse the electrochemical reduction of NO_2^- to NH_4^+, NH_2OH, and N_2O.[14] $[Ru^{III}(edta)NO]$ has been characterised using different physicochemical methods.[15–17] Recently, an X-ray structural

DOI: 10.1039/b108236c

characterisation of [Ru^{III}(edta)NO], prepared through the reaction of [Ru^{III}(edta)H_2O]$^-$ with NOCl, revealed that the edta ligand is pentadentate, with the free carboxylate arm deprotonated to balance the charge due to NO^+, which binds at the sixth position of the distorted octahedron of Ru^{III} in a linear manner.[18]

Our interest in the binding of NO to [Ru^{III}(edta)H_2O]$^-$ arises from recent studies dealing with the reversible binding of NO to metmyoglobin and selected iron(II) aminocarboxylate complexes in aqueous solution.[19,20] In these studies, Ru^{III}(edta) was used as a trap for NO in order to measure the dissociation rate constant of NO in a direct manner. We found that [Ru^{III}(edta)-H_2O]$^-$, due to its high affinity for NO and suitable chemical properties (such as a relatively high stability and oxygen insensitivity), is a promising candidate for practical application as a very efficient NO scavenger in a wide variety of trapping experiments.

The present study was undertaken to determine the stability constant and rate constants for the binding and release of NO, in order to throw more light on the intimate nature of the underlying reaction mechanism for the formation and dissociation of the [Ru^{III}(edta)NO]$^-$ complex. We wanted to achieve this goal by using two different fast kinetics techniques, *viz.* stopped-flow and laser flash photolysis. Despite all our efforts to resolve the kinetics of this reaction, of which a detailed account is given, unanswered mechanistic questions still remain.

Results and discussion

Spectroscopic studies

The UV-Vis spectrum of [Ru^{III}(edta)H_2O]$^-$ measured in 0.2 M acetate buffer solution at pH = 5.0 exhibits a band maximum at 280 nm (ε = 2800 M^{-1} cm^{-1}) and a shoulder at 350 nm (ε = 680 M^{-1} cm^{-1}). Exposure of a degassed solution of [Ru^{III}-(edta)H_2O]$^-$ to excess NO led to a significant decrease in absorbance in the range 270–410 nm and an increase in absorbance below 270 nm. Difference spectra recorded during titration of [Ru^{III}(edta)H_2O]$^-$ in aqueous solution at pH = 5.0 against a buffered NO solution (Fig. 1) indicated an isosbestic point at 271 nm. The uptake of NO appears to be irreversible as judged from experiments in which a stream of Ar was used to remove NO from solution, consistent with eqn. 3.

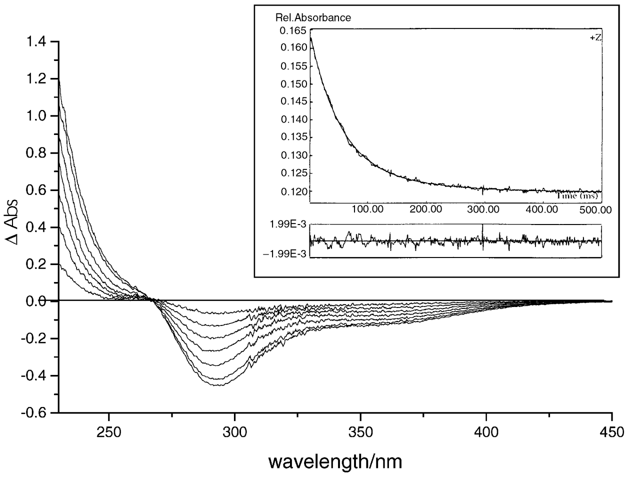

Fig. 1 Difference spectra recorded during titration of 1 × 10^{-3} M [Ru^{III}(edta)H_2O]$^-$ in aqueous solution, at pH = 5.0 with an acetate-buffered NO solution. Inset: example of a stopped-flow kinetic trace recorded for the reaction of 2.5 × 10^{-5} M [Ru^{III}(edta)H_2O]$^-$ with 1.87 × 10^{-4} M NO at 290 nm and 8 °C.

$$[\mathrm{Ru^{III}(edta)H_2O}]^- + \mathrm{NO} \longrightarrow [\mathrm{Ru^{III}(edta)NO}]^- \leftrightarrow [\mathrm{Ru^{II}(edta)NO^+}]^- \quad (3)$$

It is suggested that the formation of the nitrosyl complex is accompanied by charge transfer from NO to Ru^{III}, and the electronic configuration of the Ru^{III}–NO center may be described as Ru^{II}–NO^+. All these findings are consistent with the high value of the equilibrium constant K_{NO} determined from the spectral changes coupled to the detection of free NO using a potentiometric technique. The value of K_{NO} was found to be (9.1 ± 1.2) × 10^7 M^{-1} at 25 °C and pH = 5.0, which is 2 to 3 orders of magnitude larger than that reported in the literature for related systems.[6]

IR spectroscopy is considered to be a useful tool for the determination of the binding mode and oxidation state of NO in metal-based complexes. A vibration for coordinated NO was found at 1900 cm^{-1} for an aqueous solution of [Ru^{III}(edta)NO]$^-$ using an ATR cell. This value is in good agreement with literature values[21–23] and suggests that NO is coordinated in a linear fashion as Ru^{II}–NO^+. Further information on the nature of this complex comes from the ^{15}N-NMR measurements reported below.

Kinetic studies: stopped-flow experiments, determination of k_{on}

Recently, kinetic studies revealed that NO binds very rapidly to [Ru^{III}(edta)H_2O]$^-$ with a second-order rate constant of *ca.* 1 × 10^7 M^{-1} s^{-1} in phosphate buffer at pH = 7.4 and 7.3 °C.[5] This value was determined using stopped-flow techniques, working under second-order conditions at low concentrations of both reactants and at a low temperature.

Similar kinetic measurements on the [Ru^{III}(edta)H_2O]$^-$/NO system were performed in 0.2 M acetate buffer at pH = 5.0 and 8 °C under pseudo-first-order conditions (*i.e.* at least a sevenfold excess of NO). As can be seen from the absorbance–time plot shown in Fig. 1 (inset), complete NO binding to [Ru^{III}-(edta)H_2O]$^-$ occurs within 0.5 s with k_{obs} = 21 s^{-1} under the selected conditions. Reaction (4) is expected to follow (pseudo) first-order kinetics in the presence of a large excess of NO, to give a rate constant k_{obs} expressed as shown in eqn. (5).

$$[\mathrm{Ru^{III}(edta)H_2O}]^- + \mathrm{NO} \underset{k_{off}}{\overset{k_{on}}{\rightleftarrows}} [\mathrm{Ru^{III}(edta)NO}]^- + \mathrm{H_2O} \quad (4)$$

$$k_{obs} = k_{on}[\mathrm{NO}] + k_{off} \quad (5)$$

The plot of k_{obs} *vs.* [NO] was found to be linear with a very small intercept (Fig. 2). The slope of the line resulted in k_{on} = 1 × 10^5 M^{-1} s^{-1} at 8 °C, which is 100 times slower than that reported by Davies *et al.*[5] Different experiments were performed in an effort to resolve this apparent discrepancy.

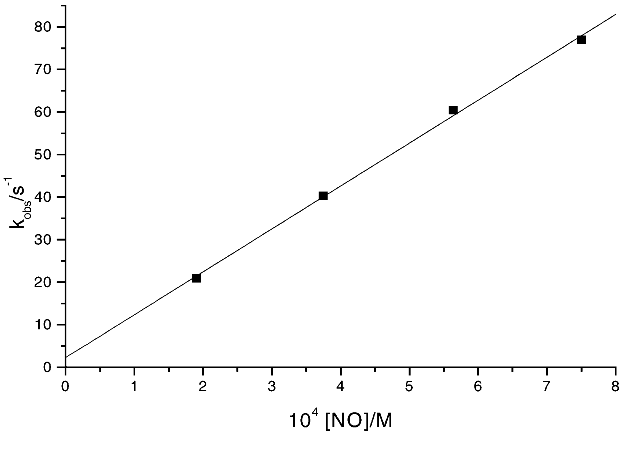

Fig. 2 Concentration dependence of k_{obs} for the binding of NO to [Ru^{III}(edta)H_2O]$^-$. Experimental conditions: [Ru^{III}(edta)H_2O^-] = 2.5 × 10^{-5} M, 0.2 M acetate buffer, pH = 5.0, 8 °C, λ = 290 nm.

Since it is practically impossible to prepare aqueous solutions of NO totally free of nitrite,[24,25] it is possible that nitrite impurities can interfere with the studied reaction and affect the value of k_{on}. For that reason, the rate constant for the reaction between $[Ru^{III}(edta)H_2O]^-$ and nitrite was determined under the same experimental conditions. As can be seen from the spectral changes recorded for the binding of nitrite to $[Ru^{III}(edta)H_2O]^-$ in 0.2 M acetate buffer solution (Fig. 3), the formation of $[Ru^{III}(edta)(NO_2)]^{2-}$ is accompanied by a significant absorbance increase in the range 250–400 nm. The kinetics of this reaction were studied by stopped-flow spectroscopy with nitrite in at least a 10-fold excess by following the absorbance changes at 290 nm. As can be seen from Fig. 3 (inset), nitrite binding to $[Ru^{III}(edta)H_2O]^-$ is significantly slower as compared to the reaction with NO and occurs with $k_{obs} = 8.39 \times 10^{-2}$ s^{-1} at 5×10^{-4} M nitrite and 8 °C. The plot of k_{obs} *vs.* $[NO_2^-]$ gives a straight line with no meaningful intercept (Fig. 4). The second-order rate constant was calculated to be $k(NO_2^-) = 169$ M^{-1} s^{-1} at 8 °C. This rate constant is 500 times slower than that determined for the reaction with nitric oxide, such that trace impurities of nitrite will not affect the NO binding kinetics.

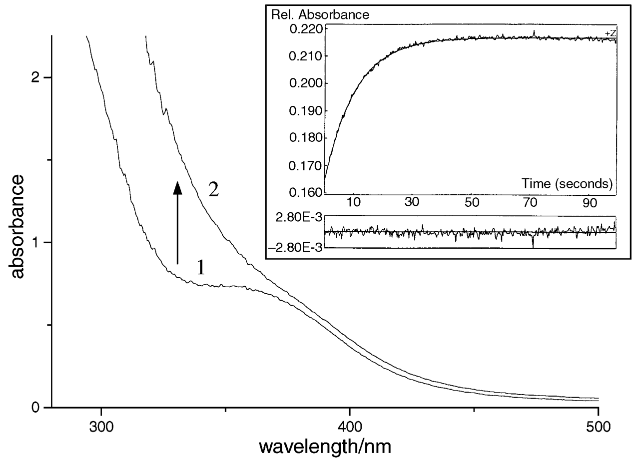

Fig. 3 Absorption spectral changes recorded for the reaction of 1×10^{-3} M $[Ru^{III}(edta)H_2O]^-$ with 1×10^{-3} M NO_2^-: (1) separate solutions, (2) after mixing. Experimental conditions: 0.2 M acetate buffer, pH = 5.0, 25 °C. Inset: example of a stopped-flow kinetic trace recorded for the reaction of 2.5×10^{-5} M $[Ru^{III}(edta)H_2O]^-$ with 5×10^{-4} M NO_2^- at 290 nm and 8 °C.

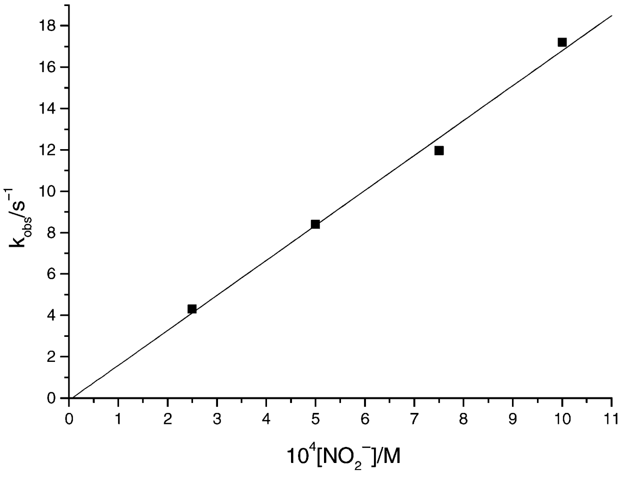

Fig. 4 Concentration dependence of k_{obs} for the binding of NO_2^- to $[Ru^{III}(edta)H_2O]^-$. Experimental conditions: $[Ru^{III}(edta)H_2O^-] = 2.5 \times 10^{-5}$ M, 0.2 M acetate buffer, pH = 5.0, 8 °C, λ = 290 nm.

The apparent discrepancy in the k_{on} values for the reaction with NO could be resolved in terms of buffer effects. It turned out that the buffer should not be present in the Ru^{III} solution, but only in the NO solution prior to mixing in the stopped-flow instrument. It is suggested that the labile water molecule in $[Ru^{III}(edta)H_2O]^-$ is substituted by an acetate ion when the complex is dissolved in the acetate buffer, according to equilibrium (6), to produce a less reactive complex.

$$[Ru^{III}(edta)H_2O]^- + Ac^- \rightleftarrows [Ru^{III}(edta)(Ac)]^{2-} + H_2O \qquad (6)$$

Experiments performed in more concentrated acetate buffer solutions (0.2, 0.4, and 1.0 M) gave practically the same value of k_{obs}. This means that under conditions where $[Ac^-] \geq 0.2$ M, $[Ru^{III}(edta)H_2O]^-$ is converted to the less labile $[Ru^{III}(edta)(Ac)]^{2-}$ complex, which undergoes a substitution reaction with NO much slower than the very labile $[Ru^{III}(edta)H_2O]^-$ species. As expected, the reaction of NO with $[Ru^{III}(edta)H_2O]^-$ carried out under the same conditions, but in the absence of a buffer, occurs extremely fast within the dead time of the stopped-flow apparatus (Fig. 5). Similar results were obtained when the buffer was added only to the NO solution, since on mixing with $[Ru^{III}(edta)H_2O]^-$, NO coordinates much faster to Ru^{III} than the acetate buffer, and prevents the interference of the latter. It follows that the rate constant reported in the literature[5] must be correct, and it is assumed that the authors followed a procedure in which the Ru^{III} complex was not in contact with the buffer prior to the reaction with NO.

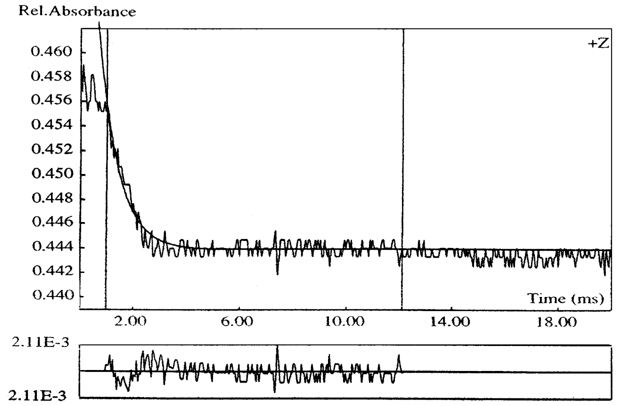

Fig. 5 Example of typical stopped-flow kinetic trace recorded for the reaction of an aqueous solution of 2.5×10^{-5} M $[Ru^{III}(edta)H_2O]^-$ with 7.5×10^{-4} M NO in 0.05 M acetate buffer, pH = 5.0, 8 °C, 290 nm.

The pH dependence of the reaction of $Ru^{III}(edta)$ with NO can reveal further information on the rate of this reaction. In aqueous solution, $Ru^{III}(edta)$ exists in three different forms, as shown in reactions (1) and (2). Each of these forms can undergo a substitution reaction with NO at very different rates, as shown in Scheme 1, based on our earlier experiences with such ligand substitution reactions.[11–13] For this reaction scheme, the overall rate expression is given by eqn. 7.

$$k_{obs} = \frac{(k_1[H^+]^2 + k_2K_1[H^+] + k_3K_1K_2)[NO]}{[H^+]^2 + K_1[H^+] + K_1K_2} \qquad (7)$$

Under limiting conditions, eqn. 7 reduces to $k_{obs} = k_1[NO]$ and $k_{obs} = k_3[NO]$ at low and high pH, respectively. This means that the pH dependence of k_{obs} should enable the determination of k_1 and k_3, since these rate constants are usually much lower than k_2 ($k_2 \sim 1 \times 10^8$ M^{-1} s^{-1} at 25 °C)[5] due to the extreme lability of $[Ru^{III}(edta)H_2O]^-$. In order to determine k_1 and k_3, kinetic measurements were performed at pH = 1.0 and 9.1, respectively.

Fig. 6 shows the spectral changes recorded for the reaction of the less labile $[Ru^{III}(edta)OH]^{2-}$ complex with NO at pH = 9.1. The $Ru^{III}(edta)$ solution was prepared in water in the absence of

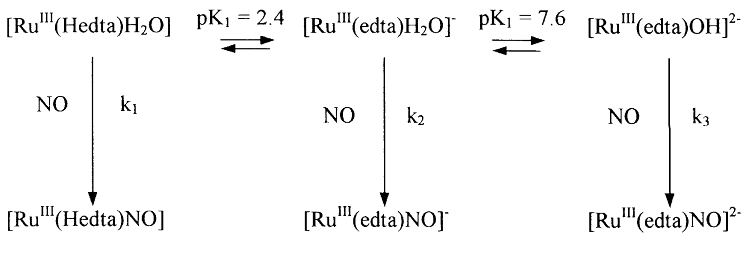

Scheme 1

buffer (pH adjusted with NaOH), whereas the NO solution contained 0.1 M Tris buffer. A typical stopped-flow trace recorded for this reaction is shown in Fig. 6 (inset). The observed rate constant was found to be 63 s^{-1} at 25 °C and 5 × 10^{-4} M NO. According to the reaction sequence shown in Scheme 1, k_{obs} at pH = 9.1 (*i.e.* at approximately a 30-fold excess of the hydroxo complex based on the quoted pK_a values) can be expressed as in eqn. (8).

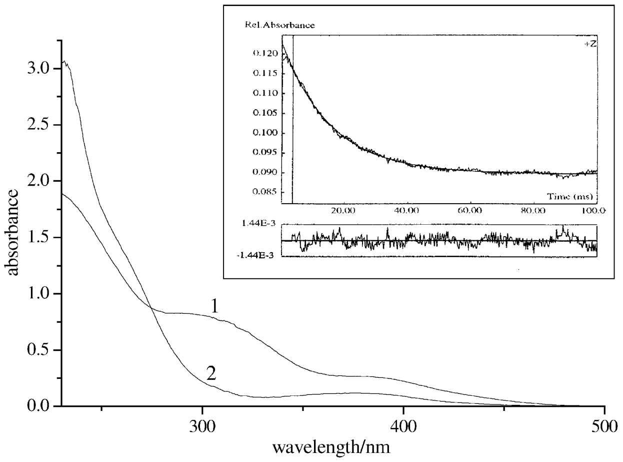

Fig. 6 Absorption spectral changes recorded for the reaction of 1 × 10^{-3} M $[Ru^{III}(edta)H_2O]^-$ with 1 × 10^{-3} M NO: (1) separate solutions, (2) after mixing. Experimental conditions: $[Ru^{III}(edta)H_2O]^-$ in aqueous solution (pH = 9.1 adjusted with NaOH), NO in 0.1 M Tris buffer, pH = 9.1, 25 °C. Inset: example of a typical stopped-flow kinetic trace recorded for the reaction of 5.0 × 10^{-5} M $[Ru^{III}(edta)H_2O]^-$ with 5.0 × 10^{-4} M NO at 310 nm and 25 °C.

$$k_{obs} = \frac{(k_2[H^+] + k_3K_2)[NO]}{[H^+] + K_2} \qquad (8)$$

In principle, it should be possible from the above equation to calculate the k_3 value, since k_{obs}, k_2 and K_2 are known. However, our attempt to determine the k_3 value in this way failed because the protonation/deprotonation rate was not taken into consideration (eqn. 9).

$$[Ru^{III}(edta)H_2O]^- \underset{k_{prot}}{\overset{k_{deprot}}{\rightleftarrows}} [Ru^{III}(edta)OH]^{2-} + H^+ \qquad (9)$$

At pH = 9.1, the protonation and deprotonation rate constants were calculated to be *ca.* 8 s^{-1} ($k_{prot}[H^+] \approx 10^{10} \times 10^{-9.1}$) and *ca.* 250 s^{-1} ($k_{deprot} = K_2k_{prot} \approx 10^{-7.6} \times 10^{10}$), respectively. Thus the protonation at pH = 9.1 is very slow, too slow to favour the aqua complex pathway, and the observed rate constant must be due to the k_3 pathway only, *i.e.* $k_3 \approx 1.2 \times 10^5$ M^{-1} s^{-1} at 25 °C.

At higher $[H^+]$ (pH < 5) it is reasonable to neglect contributions from the hydroxo pathway and in this case eqn. 7 reduces to eqn. 10.

$$k_{obs} = \frac{(k_1[H^+] + k_2K_1)[NO]}{[H^+] + K_1} \qquad (10)$$

Spectral changes recorded for NO binding to Ru^{III}(edta) at pH = 1.0 (*i.e. ca.* 25-fold excess of complex in the protonated form $[Ru^{III}(Hedta)H_2O]$) are shown in Fig. 7. The solutions of $[Ru^{III}(Hedta)H_2O]$ and NO were prepared in water and the pH adjusted with $HClO_4$. Kinetic measurements performed at pH = 1.0 using stopped-flow techniques gave k_{obs} = 18.5 s^{-1} at 25 °C and 4.5 × 10^{-4} M NO. At pH = 1.0, the protonation and deprotonation rate constants (eqn. 11) were calculated to be 10^9 s^{-1} ($k_{prot}[H^+] = 10^{10} \times 10^{-1}$)

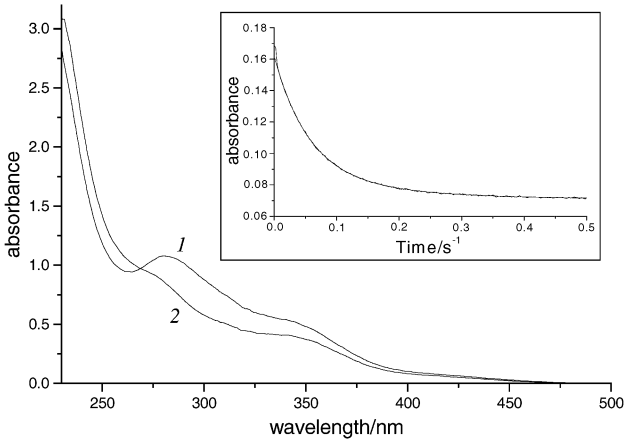

Fig. 7 Absorption spectral changes recorded for the reaction of 1 × 10^{-3} M $[Ru^{III}(edta)H_2O]^-$ with 1 × 10^{-3} M NO: (1) separate solutions, (2) after mixing. Experimental conditions: 0.1 M $HClO_4^-$, pH = 1.0, 25 °C. Inset: example of a typical stopped-flow kinetic trace recorded for the reaction of 5.0 × 10^{-5} M $[Ru^{III}(edta)H_2O]^-$ with 4.5 × 10^{-4} M NO at 290 nm and 25 °C.

$$[Ru^{III}(Hedta)H_2O] \underset{k_{prot}}{\overset{k_{deprot}}{\rightleftarrows}} [Ru^{III}(edta)H_2O]^- + H^+ \qquad (11)$$

and $10^{7.6}$ s^{-1} ($k_{deprot} = K_1k_{prot} = 10^{-2.4} \times 10^{10}$), respectively. Due to the much slower rate of deprotonation in comparison to protonation of Ru^{III}(edta) at pH = 1.0, the contribution from the k_2 pathway (eqn. 10) can be neglected and the value of k_1 calculated in this way is 3.8 × 10^4 M^{-1} s^{-1}. It follows that the k_1 and k_3 values are significantly smaller than k_2 ($k_2 \approx 1 \times 10^8$ M^{-1} s^{-1}). A similar trend was also observed for the substitution reactions of Ru^{III}(edta) with other entering nucleophiles; for instance k_1 = 130 M^{-1} s^{-1} and k_3 = 75 M^{-1} s^{-1} compared to k_2 = 1.42 × 10^3 M^{-1} s^{-1} for substitution by dimethylthiourea.[11] All of these results clearly demonstrate the much higher lability of $[Ru^{III}(edta)H_2O]^-$ as compared to $[Ru^{III}(Hedta)H_2O]$ and $[Ru^{III}(edta)OH]^{2-}$.

Determination of k_{off} by using the NO-trapping technique

The most suitable method for the direct measurement of k_{off} is to use the NO-trapping technique.[19,20] In such a case the nitrosyl complex is treated with another complex that binds NO more rapidly than the system under investigation. When an excess of the trapping complex is employed, NO release from the nitrosyl complex becomes the rate-limiting step and the observed rate constant equals k_{off}.

In the present case, $[Fe^{II}(edta)(H_2O)]^{2-}$ was used to trap NO released from $[Ru^{III}(edta)NO]^-$, since it reacts rapidly with

NO (k_{on} = 2.4 × 10^8 M^{-1} s^{-1} at pH = 5.0 and 25 °C)[20] to form the corresponding nitrosyl complex. However, under the selected conditions, the treatment of $[Ru^{III}(edta)NO]^-$ with a 20-fold excess of $[Fe^{II}(edta)(H_2O)]^{2-}$ resulted in no absorbance change that would indicate the formation of $[Fe^{II}(edta)(NO)]^{2-}$ or the aquation of $[Ru^{III}(edta)NO]^-$. Attempts to use much higher concentrations (200-fold escess) of the trapping complex also failed and, in all cases, no reaction was observed. This indicates that $[Ru^{III}(edta)H_2O]^-$ binds NO very strongly, such that k_{off} must be very small. These findings are in good agreement with the spectroscopic observations and the high value of the overall binding constant K_{NO} (> 9 × 10^7 M^{-1}).

Laser flash photolysis studies

Laser flash photolysis can be employed to study the kinetics of reactions on a significantly faster time scale than the stopped-flow technique. It was, therefore, expected to be possible to measure the value of k_{on} for the binding of NO to the most labile form of the Ru^{III}(edta) complex, *viz.* $[Ru^{III}(edta)H_2O]^-$, directly using this technique. Irradiation at 355 nm should induce the release of NO from the nitrosyl complex $[Ru^{III}(edta)NO]^-$, followed by relaxation to the original equilibrium position (Scheme 2). The rate of the reaction approaching equilibrium with one of the components (in our case NO) in large excess, is expected to follow (pseudo) first-order kinetics to give an observed rate constant (k_{obs}) expressed by eqn. 5.

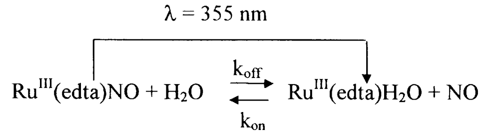

Scheme 2

All flash photolysis experiments were performed at pH = 5.0 with at least a 7-fold excess of NO. An absorbance decrease at 290 nm ascribed to relaxation to the original equilibrium position (*i.e.* re-formation of $[Ru^{III}(edta)NO]^-$) was expected following the laser flash at 355nm. However, flash photolysis experiments performed under these conditions gave unexpected results, as shown in Fig. 8. A typical kinetic trace clearly indicated multiple processes, *i.e.* two reactions occurring on the microsecond and one on the millisecond time scale [see Fig. 8(a) and (b), respectively]. Furthermore, although the flash-induced absorbance changes decayed to values close to zero (*i.e.* to the original spectrum) within 1–2 ms, residual absorbance differences still remained. It was observed that the residual spectrum decayed back to the baseline on a substantially longer time scale (20 to 30 ms). The time-resolved optical (TRO) spectra recorded during photolysis of $[Ru^{III}(edta)NO]^-$ for the short and long time scales [see Fig. 9(a) and (b)] also confirmed the occurrence of multiple chemical reaction steps. Immediately after the photolysis flash, the TRO spectra are characterized by a prompt transient absorption centered at 285 nm. The spectra collected after delays of 0.1–4.5 μs clearly show the disappearance of much of the transient absorption, accompanied by a slight shift in λ_{max} to 290 nm. Subsequently, the transient spectra decay almost back to the baseline within 1.8 ms (with an isosbestic point at 265 nm), although a significant residual spectrum remains, indicating the presence of much longer-lived species.

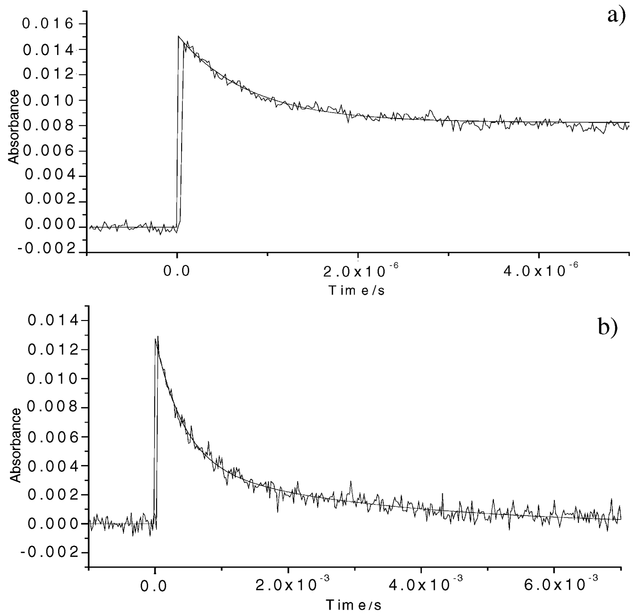

Fig. 8 Typical examples of flash photolysis kinetic traces recorded for the reaction of 2.5 × 10^{-4} M $[Ru^{III}(edta)H_2O]^-$ with 6 × 10^{-4} M NO: (a) fast reaction, (b) slow reaction. Experimental conditions: $[Ru^{III}(edta)H_2O]^-$ in aqueous solution, pH = 5.0, NO in 0.2 M acetate buffer, pH = 5.0, λ_{irr} = 355 nm, λ_{det} = 290 nm, 25 °C.

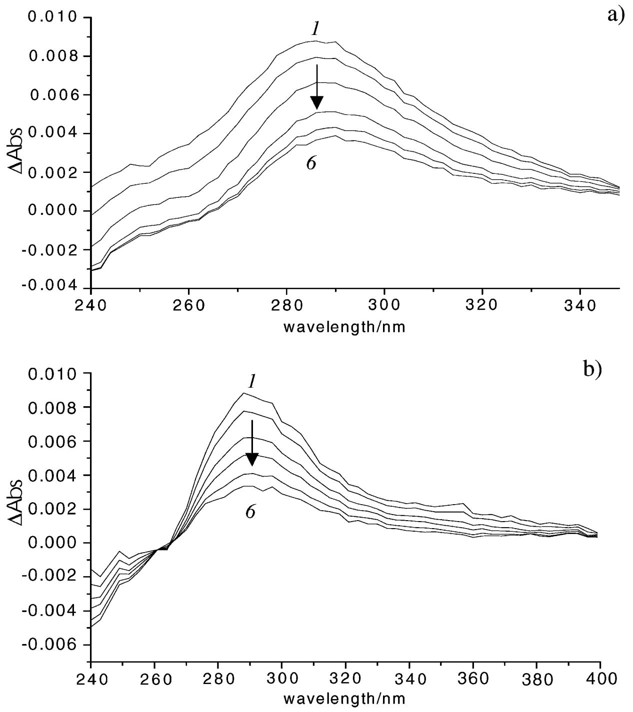

Fig. 9 Transient absorption difference spectra recorded for the $Ru(edta)(H_2O)^-$/NO system following laser flash photolysis at 355 nm. Successive measurements after delays of (a) 0.1–4.5 μs and (b) 0.1–1.8 ms. Experimental conditions: $[Ru(edta)H_2O^-]$ = 2.5 × 10^{-4} M in aqueous solution, pH = 5.0, [NO] = 1 × 10^{-3} M in 0.1 M acetate buffer, pH = 5.0, 25 °C.

These findings clearly indicate that flash photolysis of $[Ru(edta)NO]^-$ does not lead to the simple photoinduced release of NO from the nitrosyl complex followed by the re-binding of NO, as expected. In view of the fact that after the flash the transient absorption decays to re-form the initial spectrum, the possibility of a photoinduced degradation of the studied complex can be excluded. Furthermore, it was observed that while the parent Ru^{III}(edta) complex undergoes photoinduced decomposition during irradiation at 355 nm, accompanied by a significant decrease in absorbance in the range 330–412 nm (Fig. 10), flash photolysis of the nitrosyl complex (under excess NO) does not lead to such irreversible spectral changes, demonstrating the much higher photostability of the nitrosyl complex.

As can be seen from the data reported in Table 1, the rate constants determined at 290 nm and 25 °C for the three photoinduced reaction steps exhibit no meaningful NO concentration

Table 1 Rate constants determined by flash photolysis for the $[Ru^{III}(edta)H_2O]^-$/NO system[a]

T/°C	P/MPa	10^3[NO]/M	k_{obs}/s^{-1} (first reaction)	k_{obs}/s^{-1} (second reaction)	k_{obs}/s^{-1} (third reaction)
5	0.1	0.6	4.65×10^5		1.30×10^3
		1.0	4.80×10^5		1.38×10^3
		1.8	4.07×10^5		1.52×10^3
15	0.1	0.6	7.80×10^5		1.66×10^3
		1.0	7.25×10^5		2.45×10^3
		1.8	7.05×10^5		2.00×10^3
25	0.1	0.4	1.34×10^6		1.23×10^3
		0.5	1.27×10^6		1.55×10^3
		0.76	1.96×10^6	6.66×10^4	4.93×10^2
		0.95	1.69×10^6	3.23×10^4	4.40×10^3
		1.14	1.58×10^6	8.12×10^4	2.74×10^3
		1.33	1.41×10^6	6.40×10^4	4.74×10^3
		1.52	1.60×10^6	8.00×10^4	3.03×10^3
35	0.1	0.6	2.50×10^6		1.65×10^3
		1.0	2.70×10^6		2.75×10^3
45	0.1	0.6	3.98×10^6		1.40×10^4
25	10	1.0	1.20×10^6		3.50×10^3
	40		1.18×10^6		3.26×10^3
	80		9.2×10^5		4.85×10^3
	120		6.01×10^5		4.45×10^3
	160		7.10×10^5		6.87×10^3

[a] Experimental conditions: $[Ru^{III}(edta)H_2O]^-$ solution prepared in water, pH = 5.0 adjusted with NaOH, NO solution prepared in 0.2 M acetate buffer, λ_{irr} = 355 nm, λ_{det} = 290 nm.

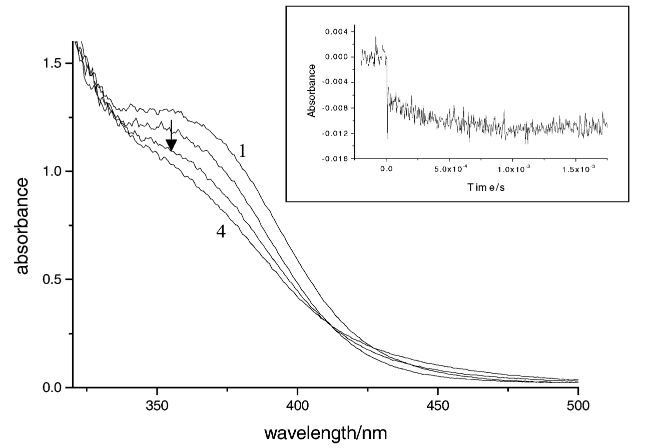

Fig. 10 Spectral changes recorded for $[Ru^{III}(edta)H_2O]^-$ following laser irradiation at λ = 355 nm: (1) before irradiation, (2–4) after 15, 30 and 45 laser flashes, respectively. Experimental conditions: 2×10^{-3} M $[Ru^{III}(edta)H_2O]^-$ in water, pH = 5.0, 25 °C. Inset: a typical kinetic trace recorded using laser flash photolysis for the decay of $[Ru^{III}(edta)H_2O]^-$ following irradiation at 355 nm.

dependence. This could be due to the fact that, because of the low solubility of NO in water, only a small range of NO concentrations could be investigated. The temperature and pressure dependence was evaluated only for the fastest and slowest steps, since extraction of rate constants for the intermediate step from the multi-exponential decay caused some difficulties and resulted in large fitting errors. The Eyring plots were found to be linear for both reactions (Fig. 11), from which the activation parameters $\Delta H^{\neq}$ and $\Delta S^{\neq}$ were determined. The values for the first reaction are $\Delta H^{\neq}$ = 36.7 ± 1.0 kJ mol^{-1} and $\Delta S^{\neq}$ = −4 ± 3 J K^{-1} mol^{-1}, and for the third reaction are $\Delta H^{\neq}$ = 17.1 ± 1.5 kJ mol^{-1} and $\Delta S^{\neq}$ = −76 ± 5 J K^{-1} mol^{-1}. The effect of pressure on these reactions results in a rather poor correlation of plots of ln(k_{obs}) *vs.* pressure (Fig. 12), but the activation volumes can nevertheless be estimated to be +10 ± 3 cm^3 mol^{-1} and −12.8 ± 1.0 cm^3 mol^{-1} for the fastest and slowest steps, respectively. The activation parameters found for the fast reaction exhibit a rather high activation enthalpy and a significantly positive activation volume, suggesting that this reaction most probably occurs according to a dissociative ligand substitution mechanism. In contrast, the slowest reaction displays a relatively low activation enthalpy, accompanied by significantly large and negative values for the activation entropy and activation volume, supporting the operation of an associative ligand substitution mechanism.

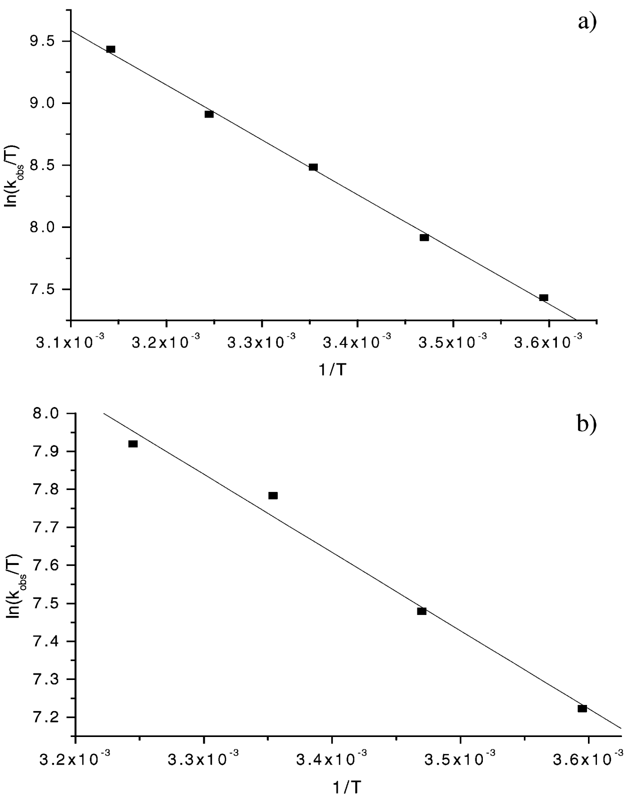

Fig. 11 Eyrings plots of ln(k_{obs}/T) *vs.* 1/T for the reaction of $[Ru^{III}(edta)H_2O]^-$ with NO: (a) first reaction, (b) third reaction. Experimental conditions: 2.5×10^{-4} M $[Ru^{III}(edta)H_2O]^-$ in water, pH = 5.0, 6×10^{-4} M NO in 0.2 M acetate buffer, λ_{irr} = 355 nm, λ_{det} = 290 nm.

It follows from this analysis that flash photolysis at 355 nm is not a suitable technique to determine kinetic data for the binding of NO to $[Ru^{III}(edta)H_2O]^-$, mainly due to the absence of an expected dependence on the concentration of NO. Since UV

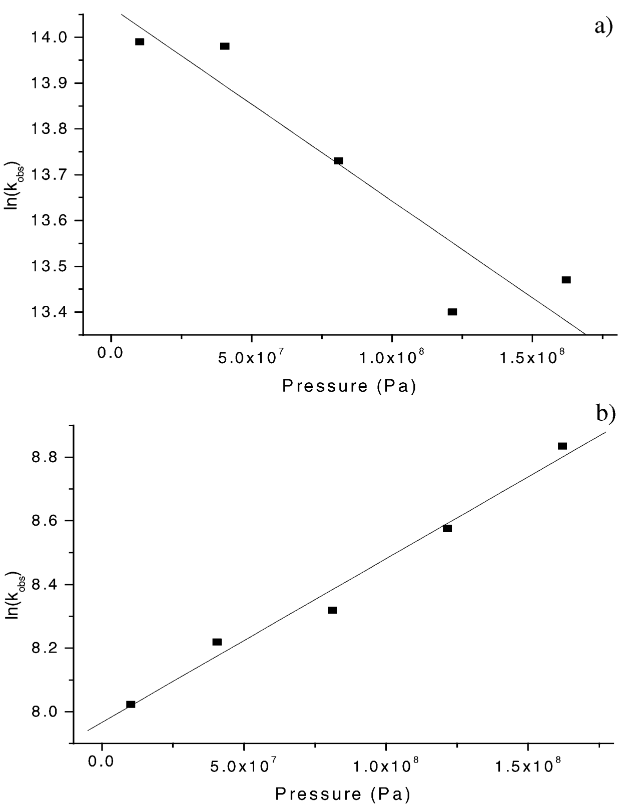

Fig. 12 Plots of $\ln(k_{obs})$ *vs.* pressure for the reaction of $[Ru^{III}(edta)H_2O]^-$ with NO: (a) first reaction, (b) third reaction. Experimental conditions: 2.5×10^{-4} M $[Ru^{III}(edta)H_2O]^-$ in water, pH = 5.0, 6×10^{-4} M NO in 0.2 M acetate buffer, 25 °C, $\lambda_{irr} = 355$ nm, $\lambda_{det} = 290$ nm.

irradiation often leads to reduction of the metal centre, it is possible that flash photolysis of $[Ru^{III}(edta)NO]^-$ at 355 nm can lead to the partial formation of Ru^{II} complexes, along with the dissociation of NO. It was not possible to repeat the flash photolysis experiments using a less reductive irradiation wavelength (*viz.* 532 nm for the present system) due to the absence of suitable spectral characteristics of $[Ru^{III}(edta)NO]^-$ in this range. The possible photo-reduction of $[Ru^{III}(edta)NO]^-$ was therefore investigated in more detail.

Laser flash photolysis of $[Ru^{II}(edta)NO]^{2-}$

In order to investigate the role of the photo-induced reduction of $[Ru^{III}(edta)NO]^-$ to $[Ru^{II}(edta)NO]^{2-}$, the reaction of Ru^{II}-(edta) with NO was studied under the same experimental conditions. As can be seen from Fig. 13, UV-Vis spectra recorded during the reduction of $[Ru^{III}(edta)H_2O]^-$ to $[Ru^{II}(edta)H_2O]^{2-}$, exhibit three isosbestic points at 270, 350 and 412 nm. In aqueous solution at pH = 5.0, $[Ru^{II}(edta)H_2O]^{2-}$ exhibits band maxima at 282 ($\varepsilon = 2900$) and 427 nm ($\varepsilon = 260$ M^{-1} cm^{-1}). In contrast to the Ru^{III} complex, $[Ru^{II}(edta)H_2O]^{2-}$ is very stable following flash irradiation at 355 nm and does not undergo photoinduced decomposition (compare insets in Fig. 10 and 13). Exposure of a degassed solution to an excess of NO led to significant loss in absorbance in the range 270–500 nm due to the formation of $[Ru^{II}(edta)NO]^{2-}$ (Fig. 14). Typical kinetic traces recorded during the flash photolysis of $[Ru^{II}(edta)NO]^{2-}$ at pH = 5.0 clearly indicate that at least two reactions occur under the selected conditions [Fig. 15(a) and (b)]. The first, very fast reaction occurs within 5 µs and the second within 1 ms. These results are similar to that observed for the Ru^{III}(edta) complex. These findings indicate that the occurrence of multiple reaction steps following 355 nm laser flash photolysis of $[Ru^{III}(edta)NO]^-$ can in part be accounted for in terms of the reduction of Ru^{III}(edta)NO to Ru^{II}(edta)NO.

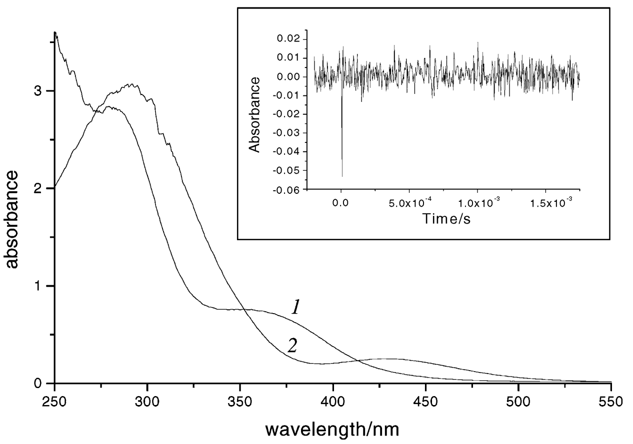

Fig. 13 Spectral changes recorded during the reduction of $[Ru^{III}(edta)H_2O]^-$ to $[Ru^{II}(edta)H_2O]^{2-}$ with zinc amalgam: (1) 1×10^{-3} M $[Ru^{III}(edta)H_2O]^-$, (2) 1×10^{-3} M $[Ru^{II}(edta)H_2O]^{2-}$. Experimental conditions: $Ru^{II/III}$(edta) solutions in water, pH = 5.0 adjusted with NaOH, 25 °C. Inset: stability of $[Ru^{II}(edta)H_2O]^{2-}$ following laser irradiation at 355 nm.

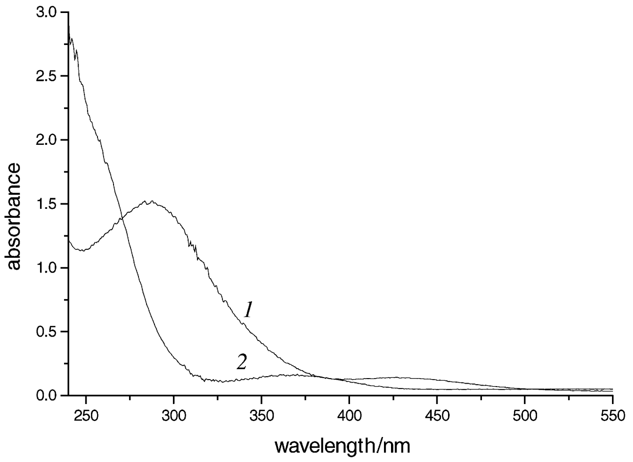

Fig. 14 Absorption spectral changes recorded for the reaction of 6.25×10^{-4} M $[Ru^{II}(edta)H_2O]^{2-}$ with 9×10^{-4} M NO: (1) separate solutions, (2) after mixing. Experimental conditions: $[Ru^{II}(edta)H_2O]^{2-}$ in aqueous solution, pH = 5.0, NO in 0.2 M acetate buffer, pH = 5.0, 25 °C.

Binding constant for $[Ru^{II}(edta)NO]^{2-}$

The stability constant for the binding of NO to $[Ru^{II}(edta)$-$H_2O]^{2-}$ (eqn. 12),

$$[Ru^{II}(edta)H_2O]^{2-} + NO \xrightleftharpoons{K_{NO}} [Ru^{II}(edta)NO]^{2-} + H_2O \quad (12)$$

can, in principle, be determined in the same way as that for the reaction of $[Ru^{III}(edta)H_2O]^-$ with NO, *i.e.* from a combination of UV-Vis spectroscopy and electrochemical detection of free NO in solution. However, for the equilibrium expressed in eqn. (12), it was difficult to determine K_{NO} accurately, since the reaction product, $[Ru^{II}(edta)NO]^{2-}$, appeared to be insufficiently stable. Accordingly, the value of the equilibrium constant for the binding of NO to $[Ru^{II}(edta)H_2O]^{2-}$ was approximately estimated to be larger than 6×10^5 M^{-1}. According to Meyer *et al.*,[26] the instability of $[Ru^{II}(edta)NO]^{2-}$ can be ascribed to disproportionation reactions such as

$$2[Ru^{II}(edta)(NO)]^{2-} \longrightarrow [Ru^{II}(edta)(NO^+)]^- + [Ru^{II}(edta)(NO^-)]^{3-} \quad (13)$$

$$2[Ru^{II}(edta)(NO^-)]^{3-} + 2H^+ \longrightarrow 2[Ru^{II}(edta)H_2O]^{2-} + N_2O \quad (14)$$

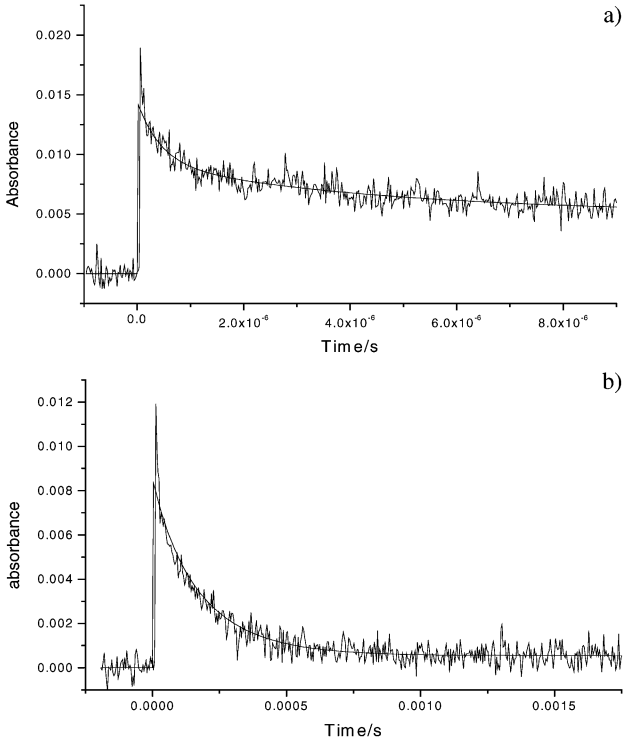

Fig. 15 Typical examples of flash photolysis kinetic traces recorded for the reaction of 2.5 × 10^{-4} M $[Ru^{II}(edta)H_2O]^{2-}$ with 9.5 × 10^{-4} M NO: (a) fast reaction, (b) slow reaction. Experimental conditions: $[Ru^{II}(edta)H_2O]^{2-}$ in aqeuous solution, pH = 5.0, NO in 0.2 M acetate buffer, pH = 5.0, λ_{irr} = 355 nm, λ_{det} = 290 nm, 25 °C.

^{15}N-NMR studies

The unexpected flash photolysis results reported above stimulated the search for more direct information on the nature of the nitrosyl complex formed during the reaction of $[Ru^{III}(edta)H_2O]^-$ with an excess of NO. ^{15}N-NMR studies were performed on aqueous solutions of $[Ru^{III}(edta)H_2O]^-$ (pH = 5.0) saturated with ^{15}NO ($Na^{15}NO_2$ reduced with ascorbic acid), using nitromethane as an external standard. As can be seen from Fig. 16, the ^{15}N-NMR spectrum exhibits two almost equally intense resonances at −17.6 and 52.4 ppm and one minor resonance at 228.5 ppm. The positions of the two main resonances are indicative of coordinated $^{15}NO^+$ and coordinated $^{15}NO_2^-$, respectively, whereas the weak resonance at 228.5 ppm indicates the presence of free $^{15}NO_2^-$ in solution.[27] This means that under the selected experimental conditions (*i.e.* in the presence of an excess of NO, and possibly NO_2^- impurities), the reaction of $[Ru^{III}(edta)H_2O]^-$ with NO does not lead to the formation of only the monosubstituted $[Ru^{II}(edta)(NO^+)]^-$ complex, but also to the disubstituted $[Ru^{II}(edta)(NO^+)(NO_2^-)]^{2-}$ complex. Labilization by coordinated NO often leads to the subsequent formation of another substitution product, that does not require the stabilization of coordinated NO, through the reduction or oxidation of the metal center, a requirement that is fulfilled with nitrite as the entering ligand.[28]

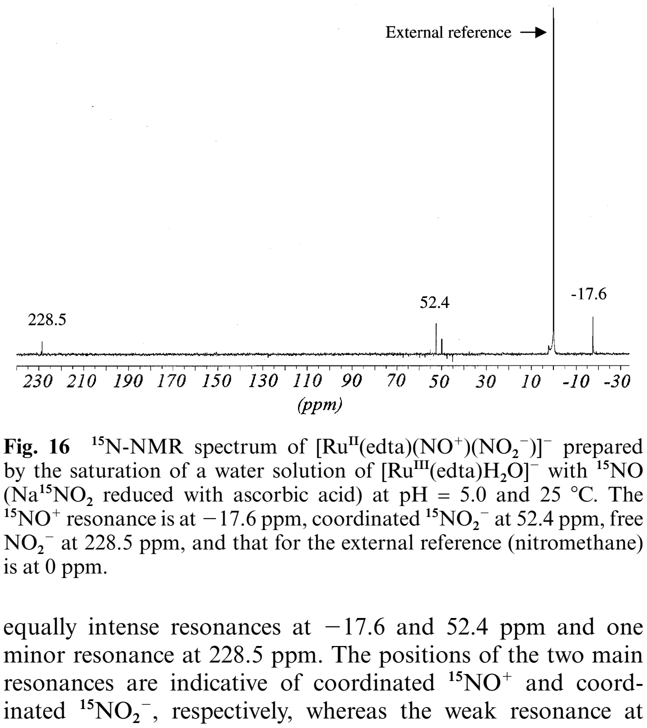

Fig. 16 ^{15}N-NMR spectrum of $[Ru^{II}(edta)(NO^+)(NO_2^-)]^-$ prepared by the saturation of a water solution of $[Ru^{III}(edta)H_2O]^-$ with ^{15}NO ($Na^{15}NO_2$ reduced with ascorbic acid) at pH = 5.0 and 25 °C. The $^{15}NO^+$ resonance is at −17.6 ppm, coordinated $^{15}NO_2^-$ at 52.4 ppm, free NO_2^- at 228.5 ppm, and that for the external reference (nitromethane) is at 0 ppm.

This suggestion is supported by the results obtained recently by Shepherd *et al.* on the related $[Ru^{II}(hedta)(NO^+)(NO_2^-)]^-$ system, where $hedta^{3-}$ = *N*-(hydroxyethyl)ethylenediaminetriacetate.[28] They showed, on the basis of ^{15}N-NMR and IR measurements, that the formation of the disubstituted $[Ru^{II}(hedta)(NO^+)(NO_2^-)]^-$ complex strongly depends on the ratio of reactants used in the reaction. For a ratio of NO_2^- : $[Ru^{II}(hedta)]^-$ = 0.81 : 1, the monosubstituted $[Ru^{II}(hedta)(NO^+)]$ complex exists as the main species in solution, whereas an excess of NO_2^- (3 : 1) causes the amount of the disubstituted complex to grow virtually to 100% of the species present in solution. Comprehensive investigations (NMR, IR, and electrochemistry)[28] enabled the authors to characterise the nature of coordinated NO in the disubstituted complexes of Ru^{II}(hedta) in more detail. In view of the fact that the NO^+ ligand is a strong π-acceptor, it is not surprising that its binding to the metal center of aminocarboxylate complexes will promote the labilization of one *cis* in-plane carboxylate moiety and lead to the formation of the disubstituted complex. The attachment of NO_2^- to the Ru^{II} center probably occurs through N as the donor atom, since the N-bound form can participate in both σ and π bonding to the metal center. The IR studies clearly confirmed this assumption.[28] The similarity between the $[Ru^{II}(hedta)(NO^+)(NO_2^-)]^-$ and $[Ru^{II}(edta)(NO^+)(NO_2^-)]^{2-}$ complex ions leads to the suggestion that the nitrite ligand in the latter complex is also attached through N and not through O as the donor atom to the Ru^{II} centre.

Explanation offered for the multi-step reactions observed during flash photolysis

The finding that the principal product of the reaction of $[Ru^{III}(edta)H_2O]^-$ with an excess of NO is the disubstituted complex $[Ru^{II}(edta)(NO^+)(NO_2^-)]^{2-}$, enabled a clarification of the results obtained from the flash photolysis studies. In this respect, it should be noted that the flash photolysis of the related nitrosyl nitrito complexes Ru^{II}(Por)(NO)(ONO) (Por = model porphyrins) was recently studied by Ford *et al.*[29] They found that flash photolysis of ruthenium nitrosyl nitrito complexes results in multiple reaction steps, which are ascribed to the prompt formation of two primary photoproducts, *viz*. Ru^{II}(Por)(ONO) and Ru^{II}(Por)(NO), that decay at different rates to regenerate the starting complex.

These results are consistent with our observations on the $[Ru^{II}(edta)(NO^+)(NO_2^-)]^{2-}$ system. The TRO spectra recorded on the short time scale (0.1–4.5 μs) clearly indicate the prompt formation of more than one primary photoproduct. This is confirmed by two parallel exponential decays of the transient absorbance change recorded on the microsecond time scale at 290 nm. The formation of two photo-produced intermediates may occur along two pathways (see Scheme 3). One of these involves photodissociation of NO from $[Ru^{II}(edta)(NO^+)(NO_2^-)]^{2-}$ to give $Ru^{III}(edta)(NO_2^-)$, which reacts rapidly (k_{obs} ~ 10^6 s^{-1}) with excess NO to regenerate the starting complex. A second pathway involves photodissociation of NO_2 to give $[Ru^{II}(edta)(NO)]^{2-}$, which is trapped by excess NO (k_{obs} ~ 10^4 s^{-1}) to form the longer-lived dinitrosyl complex, $[Ru^{II}(edta)(NO)_2]^{2-}$. This complex subsequently reacts (k_{obs} ~ 10^3–10^2 s^{-1})

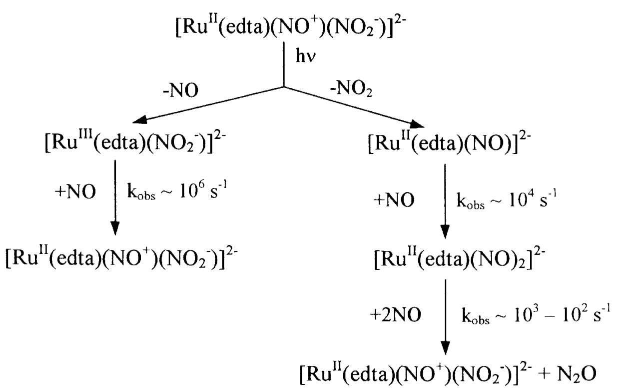

Scheme 3

with NO to regenerate [Ru^{II}(edta)(NO$^+$)(NO$_2^-$)]$^{2-}$. The TRO spectra recorded after delays of 0.1–1.8 ms [see Fig. 9(b)] exhibit an isosbestic point at 265 nm ascribed to the conversion of the dinitrosyl to the starting complex. The suggested reactions are expected to exhibit a dependence on the concentration of NO in solution, which was not observed (see Table 1). This can only mean that either the limited concentration range that could be selected in these experiments is not sufficient to show this dependence, or that the re-binding of NO follows a limiting D mechanism, *i.e.* an NO concentration independent pathway. In fact, a number of cases are now known where binding of NO to a metal center indeed follows a dissociative mechanism[19,30,31] and is, in some cases, controlled by the rate and mechanism of water exchange on the metal center.[31,32] In the present case, this suggestion would mean that the photo-generated species rapidly bind solvent water molecules prior to the displacement by NO, that will then follow a dissociative mechanism. In light of the activation parameters found in the present study for the rapid photo-induced reaction, which support the operation of a dissociative mechanism, we presently prefer the latter interpretation of the kinetic data.

The third reaction, representing the slow conversion of the dinitrosyl complex to the starting nitrosyl nitro complex can be best described by an associative mechanism based on the large and negative values of $\Delta S^{\neq}$ and $\Delta V^{\neq}$. This mechanism seems to be in good agreement with that proposed previously by Ford *et al.* to account for the formation of nitrosyl nitrito complexes of the type Ru(Por)(NO)(ONO).[33] According to this mechanism, the metal center serves as a template for the assembly of several NO equivalents that then can decompose to nitrous oxide and coordinated NO$_2$. Such a disproportionation pathway also seems to be possible in the studied case. However, in view of the fact that the slow reaction exhibits no NO concentration dependence, acceptance of this mechanism awaits further evidence.

Conclusions

Nitric oxide binds rapidly to [Ru^{III}(edta)H$_2$O]$^-$ to form a very stable nitrosyl complex, characterized by a high complex-formation constant and a very small dissociation rate constant. The complex-formation reaction (k_{on}) is extremely fast and occurs within the dead time of the stopped-flow instrument. Acetate buffer can interfere with this reaction and cause much slower complex formation with NO. The [Ru^{III}(edta)H$_2$O]$^-$ complex is an ideal and versatile scavenger for NO. Attempts to determine the complex-formation rate constant (k_{on}) using laser flash photolysis techniques were complicated due to the occurrence of unwanted side reactions.

The lower limit of the stability constant for the [Ru^{III}(edta)-NO]$^-$ complex was experimentally found to be K_{NO}(Ru^{III}) ≥ 9 × 10^7 M^{-1}. This value is in good agreement with the K_{NO}(Ru^{III}) value calculated on the basis of a Born–Haber-type cycle using the electrochemical[26] and thermodynamic data for the [Ru$^{II/III}$(edta)H$_2$O]$^{2-/-}$ and [Ru$^{II/III}$(edta)(NO)]$^{2-/-}$ couples (see Scheme 4). Based on these data, the value of the equilibrium constant for the binding of NO to [Ru^{III}(edta)H$_2$O]$^-$ can be determined from the following expression:

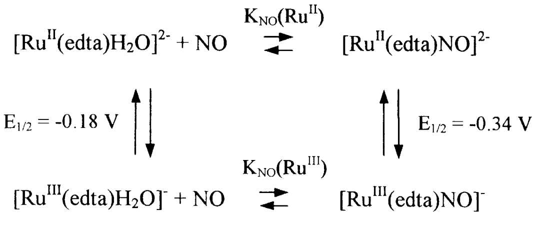

Scheme 4

$$K_{NO}(\mathrm{Ru^{III}}) = K_{NO}(\mathrm{Ru^{II}})/\exp(nF\Delta E/RT) \qquad (15)$$

Since K_{NO}(Ru^{II}) was experimentally found to be larger than 6 × 10^5 M^{-1}, the K_{NO}(Ru^{III}) value can thus be calculated to be ≥ 3 × 10^8 M^{-1}, which is in good agreement with the experimental value.

Experimental

Materials

K[Ru(Hedta)Cl]·2H$_2$O was prepared from K$_2$[RuCl$_5$(H$_2$O)] as described in the literature.[34] The complex was characterised by using spectroscopic (UV-Vis) and analytical techniques. All other chemicals were of analytical reagent grade, and deionized water was used throughout this study. Acetate (Aldrich) and 2-amino-2-(hydroxymethyl)-1,3-propanodiol (Tris, Sigma Chemicals) buffers were used to control the pH of the test solutions at pH = 5.0 and 9.0, respectively. The pH was adjusted by addition of hydrochloric acid (Titrisol, Merck) or sodium hydroxide. [Ru^{II}(edta)H$_2$O]$^{2-}$ was prepared in aqueous solution (pH = 5.0) by the reduction of [Ru^{III}(edta)H$_2$O]$^-$ with zinc amalgam.

All experiments were performed under strict exclusion of oxygen. Buffer solutions were deaerated for extended periods (in general, 1 min per mL of solution) with pure N$_2$ or Ar before they were brought in contact with the Ru^{III} and Fe^{II} complexes or nitric oxide; in some cases, freeze–thaw cycles were performed under vacuum in order to completely remove the dissolved oxygen from the solution. A stock solution of nitric oxide was prepared in a gas-tight syringe by degassing a buffer solution, followed by saturation with nitric oxide to a final NO concentration of 1.9 × 10^{-3} M at 23 °C. Dilutions of known concentration were prepared from this saturated solution by the use of a syringe technique. Nitric oxide gas was purchased as commercially available NO bottles (Linde 93 and Riessner) and cleaned of traces of higher nitrogen oxides, such as N$_2$O$_3$ and NO$_2$, by passing the gas through an Ascarite II column and then bubbling through a gas scrubbing bottle containing 5 M NaOH. A second scrubbing bottle with water was used to prevent aerosol contamination. The whole system was purged with oxygen-free argon to remove residual oxygen.

Measurements

pH measurements were performed on a Metrohm 623 pH meter with a Sigma glass electrode or on a Mettler Delta 340 pH meter. The concentration of free NO in solution was determined with an ISO-NOP electrode connected to an ISO-NO Mark II NO sensor from World Precision Instruments. The NO electrode was calibrated daily with fresh solutions of sodium nitrite and potassium iodide, according to the method suggested by the manufacturers. The determination of the stability constant K_{NO} was performed as described elsewhere.[35]

UV-Vis spectra were recorded on a Shimadzu UV-2100 spectrophotometer equipped with a thermostated cell compartment CPS-260. IR spectra were recorded using a two-mirror ATR cell on a ATI Mattson FTIR Infinity spectrophotometer. The reflection instrument utilizes a Ge crystal as an internal reflection plate with a size of 50 × 20 × 2 mm and 45° angle of incidence. For the nitrosyl complex, four independent measurements of 100 scans each were performed under inert gas atmosphere.

^{15}N-NMR spectra were recorded on a Bruker Avance DRX400 WB spectrometer at 40.56 MHz. Neat nitromethane was used as an external reference standard. ^{15}N-enriched [Ru^{III}(edta)^{15}NO] was prepared by the reduction of Na^{15}NO$_2$ with ascorbic acid to produce ^{15}NO, which was brought in contact with the edta complex of Ru^{III}. The pH of the solution was carefully adjusted to the desired value with deoxygenated NaOH or HClO$_4$ under nitrogen atmosphere. Formation of the nitrosyl complex was confirmed by the UV-Vis spectrum of a diluted sample.

Kinetic measurements were performed by rapidly mixing solutions of Ru$^{III/II}$ complexes with solutions of NO (or NaNO$_2$) using a SX-18·MV (Applied Photophysic) stopped-flow spectrometer. The changes in absorbance were monitored at 290 nm. All stopped-flow experiments were performed under pseudo-first-order conditions and the reported rate constants are the mean values from at least five kinetic runs.

Laser flash photolysis kinetic studies were carried out using a LKS·60 spectrometer from Applied Photophysics for detection and a Nd: YAG laser (SURLITE I-10 Continuum) pump source operating in the third harmonic (λ_{exc} = 355 nm; 100 mJ pulses with *ca.* 7 ns pulse widths). Spectral changes at 290 nm were monitored using a 100 W Xenon arc lamp, a monochromator, and a PMT-1P22 photomultiplier tube. The absorbance reading was balanced to zero before the flash, and data were recorded on a DSO HP 54522A digital storage oscilloscope and then transferred to a computer for subsequent analysis. Gas-tight quartz cuvettes and a pill-box cell combined with high pressure equipment[36] were used at ambient and under high pressure (up to 170 MPa), respectively. At least 30 kinetic runs were recorded under all conditions, and the reported rate constants represent the mean values of these.

Acknowledgements

The authors gratefully acknowledge financial support from the Deutsche Forschungsgemeinschaft and the Max-Buchner-Forschungsstiftung. Studies at the Jagiellonian University were supported by the State Committee for Scientific Research, Poland, KBN (3TO9A11515 and 1605/T09/2000/19) and the Foundation for Polish Science (“Fastkin” no. 8/97).

References

1 M. J. Clarke and J. B. Gaul, *Struct. Bonding*, 1993, **81**, 147.
2 S. P. Fricker, E. Slade, N. A. Powell, O. J. Vaughan, G. R. Henderson, B. A. Murrer, I. L. Megson, S. K. Bisland and F. W. Flitney, *Br. J. Pharmacol.*, 1997, **122**, 1441.
3 Y. Chen, F.-T. Lin and R. E. Shepherd, *Inorg. Chem.*, 1999, **38**, 973.
4 S. P. Fricker, *Platinum Metals Rev.*, 1995, **39**, 150.
5 N. A. Davies, M. T. Wilson, E. Slade, S. P. Fricker, B. A. Murrer, N. A. Powell and G. R. Henderson, *Chem. Commun.*, 1997, 47.
6 T. Matsubara and C. Creutz, *Inorg. Chem.*, 1979, **18**, 1956.
7 H. Taube, *Comments Inorg. Chem.*, 1981, **1**, 17 and references cited therein.
8 I. Rapaport, L. Helm, A. E. Merbach, P. Bernhard and A. Ludi, *Inorg. Chem.*, 1988, **27**, 873.
9 H. E. Toma, P. S. Santos, M. P. D. Mattioli and L. A. A. Oliveira, *Polyhedron*, 1987, **6**, 603.
10 H. Ogino and M. Shimura, *Adv. Inorg. Bioinorg. Mech.*, 1986, **4**, 107.
11 H. C. Bajaj and R. van Eldik, *Inorg. Chem.*, 1988, **27**, 4052.
12 H. C. Bajaj and R. van Eldik, *Inorg. Chem.*, 1988, **28**, 1980.
13 H. C. Bajaj and R. van Eldik, *Inorg. Chem.*, 1990, **29**, 2855.
14 M. R. Rhodes, M. H. Barley and T. J. Meyer, *Inorg. Chem.*, 1991, **30**, 629.
15 E. Diamantis and J. V. Dubrawski, *Inorg. Chem.*, 1981, **20**, 1142.
16 J. Lewis, R. J. Irwing and G. Wilkinson, *J. Inorg. Nucl. Chem.*, 1958, **7**, 32.
17 A. Abraham and B. Bianey, *EPR of Transition Metal Ions*, Clarendon Press, Oxford, 1970.
18 M. M. T. Khan, K. Venkatasubramanian, Z. Shirin and M. M. Bhadbhade, *J. Chem. Soc., Dalton Trans.*, 1992, 1031.
19 L. E. Laverman, A. Wanat, J. Oszajca, G. Stochel, P. C. Ford and R. van Eldik, *J. Am. Chem. Soc.*, 2001, **123**, 285.
20 T. Schneppensieper, A. Wanat, G. Stochel, S. Goldstein, D. Meyerstein and R. van Eldik, *Eur. J. Inorg. Chem.*, 2001, 2317.
21 S. S. S. Borges, C. U. Davanzo, E. E. Castellano, J. Z-Schpector, S. C. Silva and D. W. Franco, *Inorg. Chem.*, 1998, **37**, 2670.
22 E. E. Mercer, W. A. Mcallister and J. R. Durig, *Inorg. Chem.*, 1966, **5**, 1881.
23 J. B. Godwin and T. J. Meyer, *Inorg. Chem.*, 1971, **10**, 471.
24 H. H. Awad and D. M. Stanbury, *Int. J. Chem. Kinet.*, 1993, **25**, 375.
25 M. Feelish, *J. Cardiovasc. Pharmacol.*, 1991, **17**, 25.
26 M. R. Rhodes, M. H. Barley and T. J. Meyer, *Inorg. Chem.*, 1991, **30**, 629.
27 (*a*) D. M. P. Mingos and D. J. Sherman, *Adv. Inorg. Chem.*, 1989, **34**, 293; (*b*) R. Bramley, B. N. Figgis and R. S. Nyholm, *J. Chem. Soc. A*, 1967, 861.
28 Y. Chen, F.-T. Lin and R. E. Shepherd, *Inorg. Chem.*, 1999, **38**, 973.
29 I. M. Lorković, K. M. Miranda, B. Lee, S. Bernhard, J. R. Schoonover and P. C. Ford, *J. Am. Chem. Soc.*, 1998, **120**, 11674.
30 L. E. Laverman, M. Hoshino and P. C. Ford, *J. Am. Chem. Soc.*, 1997, **119**, 12663.
31 T. Schneppensieper, A. Wanat, G. Stochel and R. van Eldik, *Inorg. Chem.*, in press.
32 T. Schneppensieper, A. Zahl and R. van Eldik, *Angew. Chem.*, 2001, **113**, 1727.
33 I. M. Lorković and P. C. Ford, *Inorg. Chem.*, 1999, **38**, 1467.
34 A. A. Diamantis and J. V. Dubrawski, *Inorg. Chem.*, 1981, **20**, 1142.
35 T. Schneppensieper, S. Finkler, A. Czap, R. van Eldik, M. Heus, P. Nieuwenhuizen, C. Wreesmann and W. Abma, *Eur. J. Inorg. Chem.*, 2001, 491.
36 M. Spitzer, F. Gartig and R. van Eldik, *Rev. Sci. Instrum.*, 1988, **59**, 2092.